Statistical Analysis of WDM Model Predictions and Observational Data Conformance Incorporating Velocity Factors

General Approach

In this work we aim to obtain quantitative conclusions about WDM cosmologies through a statistical analysis of Milky Way satellite properties. This work follows a nearly identical process to Ref. [1] applied to WDM models. As in [1], we include in our calculations the half-light radius, stellar velocity dispersion, and total number of classical and SDSS Milky Way satellites, using the observational data collected in [2]. Due to baryonic effects and significant tidal stripping potentially skewing our results, we have excluded the Magellanic clouds, Pisces II, and Sagittarius from our analysis (they would have composed $< 13\%$ of our sample so omitting them should not have a large effect) [1]. We assign a thermal relic mass to characterize each WDM model. Throughout this statistical analysis we compute the likelihood function for each WDM model for thermal relic masses between 1-12keV/c^2,

$$-2\ln\mathcal{L} = -2\sum_i \ln\mu(\sigma_{\rm los}^{*\,{\rm obs,\,i}}, R_{\rm eff}^{\rm obs,\,i}) - 2\ln\mathcal{P}(N_{\rm obs}) - 2\ln\mathcal{N}_{\sigma_{C_\Omega}}(1,\,0.19). \tag{1}$$

As in [1], $\mu(\sigma_{\rm los}^{*\,\rm obs}, R_{\rm eff}^{\rm obs})\mathrm{d}\sigma_{\rm los}^{*\,\rm obs}\mathrm{d}R_{\rm eff}^{\rm obs}$ is the differential probability for a satellite galaxy to have an observed line of sight stellar velocity dispersion $\sigma_{\rm los}^{*\,\rm obs}$ and 2D half-light radius $R_{\rm eff}^{\rm obs}$. $\sigma_{\rm los}^{*\,\rm obs,\,i}$ and $R_{\rm eff}^{\rm obs,\,i}$ are the stellar velocity dispersions and half-light radii respectively of the i$^{\rm th}$ observed Milky Way satellite galaxy. $\mathcal{P}(N_{\rm obs})$ is the probability to observe $N_{\rm obs}$ satellite galaxies, with $N_{\rm obs} = 21$ the true number of observed Milky Way satellite galaxies (after omitting the three mentioned above). $\mathcal{N}_{\sigma_{C_\Omega}}(1,\,0.19)$ is a Gaussian centered on 1 with width 0.19 included to account for σ_{C_Ω}, the scatter associated with the anisotropy of the Milky Way satellite distribution (we expand on this further below).

Method to Compute $\mu(\sigma_{\rm los}^{*\,\rm obs,\,i}, R_{\rm eff}^{\rm obs,\,i})$

The first probability is given by [1]

$$\mu(\sigma_{\rm los}^{*\,\rm obs}, R_{\rm eff}^{\rm obs}) = \int \mathcal{P}(\sigma_{\rm los}^*, R_{\rm eff}, c, M_*, M)\frac{1}{\sqrt{2\pi}\Delta\sigma}e^{(-\frac{(\sigma_{\rm los}^{*\,\rm obs}-\sigma_{\rm los}^*)^2}{2(\Delta\sigma)^2})}\frac{1}{\sqrt{2\pi}\Delta R_{\rm eff}}e^{(-\frac{(R_{\rm eff}^{\rm obs}-R_{\rm eff})^2}{2(\Delta R_{\rm eff})^2})}\mathrm{d}\sigma_{\rm los}^*\,\mathrm{d}R_{\rm eff}\,\mathrm{d}c\,\mathrm{d}M_*\,\mathrm{d}M. \tag{2}$$

Where $\mathcal{P}(\sigma_{\rm los}^*, R_{\rm eff}, c, M_*, M)\mathrm{d}\sigma_{\rm los}^*\,\mathrm{d}R_{\rm eff}\,\mathrm{d}c\,\mathrm{d}M_*\,\mathrm{d}M$ is the differential probability to observe a Milky Way satellite galaxy with true line of sight stellar velocity dispersion $\sigma_{\rm los}^*$, 2D half-light radius $R_{\rm eff}$, concentration c, stellar mass M_*, and DM halo mass M. We use the "200c" convention for M (where a dark matter halo is defined out to the radius where the density is 200 times the critical density of the universe) and take the concentration as

$$c_{200_{\rm c}} \equiv r_{\rm vir}/r_{\rm s}, \tag{3}$$

with $r_{\rm s}$ the scale radius of the NFW profile whose functional form is given in Ref. [3]. Following [1], we simplify by assuming Gaussian uncertainties in $\sigma_{\rm los}^*$ and $R_{\rm eff}$. The two Gaussians, with $\Delta\sigma$ and $\Delta R_{\rm eff}$ signifying the observational uncertainties, indicate the probabilities of observing a velocity dispersion $\sigma_{\rm los}^{*\,\rm obs}$ and half-light radius $R_{\rm eff}^{\rm obs}$, given their real values, $\sigma_{\rm los}^*$ and $R_{\rm eff}$, respectively. As in [1], we cautiously disregard correlations between $\Delta\sigma$ and $\Delta R_{\rm eff}$ and are able to include non-Gaussian uncertainty should evidence of correlation arise.

Conditional Probabilities

As in [1], the probability from Eq. 2 can be reduced using conditional probabilities:

$$\begin{aligned}\mathcal{P}(\sigma^*_{\rm los}, R_{\rm eff}, c, M^*, M) &= \mathcal{P}(\sigma^*_{\rm los}, R_{\rm eff}, c, M^*|M)\mathcal{P}(M)\\ &= \mathcal{P}(\sigma^*_{\rm los}, R_{\rm eff}|c, M_*, M)\mathcal{P}(c, M_*|M)\mathcal{P}(M)\\ &= \mathcal{P}(\sigma^*_{\rm los}|R_{\rm eff}, c, M_*, M)\mathcal{P}(R_{\rm eff}|c, M_*, M)\mathcal{P}(c, M_*|M)\mathcal{P}(M),\end{aligned} \tag{4}$$

where

- $\mathcal{P}(M)$, the probability to observe a satellite galaxy with DM halo mass M, is the product of the subhalo mass function at infall redshift, the halo occupation fraction, and the WDM transfer function [1]. We approximate the subhalo mass function as

$$\mathrm{f}_{\rm subhalo}(M) = M^{-1.84}, \tag{5}$$

  following Table 1 in Ref. [4] with M the infall mass [5]. As in [1] we take the halo occupation fraction to be

$$\mathrm{hof}(M) = \frac{1+\mathrm{erf}(\alpha^{\rm hof}\log_{10}[M/M_0^{\rm hof}])}{2}, \tag{6}$$

  with erf the error function. $\alpha^{\rm hof} > 1$ [6, 7] is a parameter that regulates how sharp the transition is and $M_0^{\rm hof}$ is a parameter that sets the threshold mass below which halos do not host galaxies. As in [1] we take $\alpha^{\rm hof} = 1.3$ and $M_0^{\rm hof} = 10^{8.35}\mathrm{M}_\odot$ as a result of semi-analytic modelling and simulation work done in Refs. [4, 5]. The WDM transfer function is parameterized as [8]

$$\mathrm{f}_{\rm transfer}(M) = 1 + \left[4.2\left(\frac{M_{\rm hm}}{M}\right)^{2.5}\right]^{-0.2}, \tag{7}$$

  with $M_{\rm hm}$ the half-mode mass [9].

- Following [1], we assume that $R_{\rm eff}$ only depends on stellar mass (as a result of the observational results in [10]). Thus, $\mathcal{P}(R_{\rm eff}|c, M_*, M)$ can be simplified to $\mathcal{P}(R_{\rm eff}|M_*)$. We take $\mathcal{P}(R_{\rm eff}|M_*)$ to be a lognormal distribution with median $R_{\rm eff} = 0.021M_*^{0.239}$ and scatter of 0.234 dex [10]. As in [1], the stellar mass-halo mass relation is the only correlation between $R_{\rm eff}$ and M, therefore observational uncertainties do not significantly impact the net error.

- Following [1], we assume that c and M_* are independent and only related to M. Thus, $\mathcal{P}(c, M_*|M)$ can be reduced to $\mathcal{P}(c|M)\mathcal{P}(M_*|M)$. Then,

  – $\mathcal{P}(c|M)$ is given as a lognormal distribution with median computed as

$$c_{\rm WDM} = c_{\rm CDM}\left[1 + 15\left(\frac{M_{\rm hm}}{M_{\rm 1m}}\right)\right]^{0.3}, \tag{8}$$

  following the relation from [11], and scatter of 0.16 dex [12]. $M_{\rm hm}$ is the WDM half mode mass [9] and $M_{\rm 1m}$ is the halo mass defined using the "1m" convention. We convert to "1m' from "200c" using Colossus [13]. As in [1], $c_{\rm CDM}$ (the CDM concentration), is taken to be a lognormal distribution with median given by [14] and 16% lognormal scatter [12].

– Following [1], $\mathcal{P}(M_*|M)$ is the product of the completeness correction probability $\mathcal{P}_{\rm obs}$ and the stellar mass-halo mass relation probability. The completeness correction takes into account that not all halos hosting galaxies are observable by a given survey (surveys often miss faint and distant galaxies). For the completeness correction, we utilize the following relations from [15]:

$$\begin{aligned}\mathcal{P}_{\rm obs} &= \frac{\int_{V_{\rm obs}(L)} n(\vec{r})\mathrm{d}^3 r}{\int_{V_{\rm vir}(L)} n(\vec{r})\mathrm{d}^3 r} \equiv \frac{1}{\mathcal{C}(L)} \ ; \ \mathcal{C}(L) \equiv \mathcal{C}_\Omega \mathcal{C}_r \ ; \\ \mathcal{C}_\Omega &\equiv \frac{4\pi}{\Omega} \ ; \ \mathcal{C}_r \equiv \frac{\int_0^{r_{\rm vir}} n(r)\mathrm{d}^2 r}{\int_0^{r_{\rm c}(L)} n(r)\mathrm{d}^2 r} \ ; \ r_{\rm c}(L) = 1.5{\rm kpc}(L/L_\odot)^{0.51},\end{aligned} \tag{9}$$

with n the number density of satellites, $V_{\rm vir}$ the virial volume of the Milky Way, $V_{\rm obs}(L)$ the volume where satellites of luminosity L can be detected by the survey. $\mathcal{C}(L)$ is the luminosity-dependent completeness correction [15]. We assume that $n(\vec{r})$ does not change considerably with the solid angle, as in [1]. As a result, the selection function may be divided into two components, a radial component ($\mathcal{C}_{\rm r}$) and an angular component ($\mathcal{C}_\Omega$). Ω is the angular coverage of the survey, $r_{\rm vir}$ is the Milky Way virial radius, and $r_{\rm c}(L)$ is the largest distance at which satellites of luminosity L can be observed by the survey [16, 17]. Both classical and SDSS satellites are taken into account; for the latter, $\Omega_{\rm SDSS} = 3.65$sr. Assuming $M_*/M_\odot = 2L/L_\odot$ (which is suitable for older stellar populations [18, 19]), we calculate luminosities. We also assume Milky Way virial mass of $10^{12}\,M_\odot$ and Milky Way concentration of 9 [20], and we use Colossus to compute the Milky Way virial radius [13].

The completeness correction could also depend on $R_{\rm eff}$ (due to the link between $R_{\rm eff}$ and surface brightness) [21] but this correction is minimal because of the extent of uncertainties related to the halo occupation fraction, stellar mass-halo mass relation, and completeness correction [1]. Following [1] we include anisotropy-induced scatter as mentioned above: we multiply $\mathcal{C}_\Omega$ by a parameter $\sigma_{\mathrm{C}_\Omega}$, and we add a Gaussian function, $\mathcal{N}(1, 0.19)$, to the the likelihood function (Eq. 1) to represent $\sigma_{\mathrm{C}_\Omega}$ [22] (this is a safe approximation that was calculated before the completion of SDSS.). As in [1], due to the effects of tidal disruption, we set $n(r)$, the spatial satellite distribution function, to interpolate between the NFW profile, $n_{\rm NFW}(r)$, and the tidally disrupted profile, $n_{\rm GK17}(r)$, from [23],

$$n(r) = n_{\rm GK17}(r) + y_{\rm C}[n_{\rm NFW}(r) - n_{\rm GK17}(r)], \tag{10}$$

with $y_{\rm C} \in [0, 1]$ the interpolation parameter. The latter distribution decreases the density of subhalo occurrences within the inner ~ 100 kpc. Following [1], we assume that any increase in subhalo abundance within the inner ~ 50 kpc due to recent movement of the Large Magellanic Cloud [24, 25] is negligible compared to the tidal disruption uncertainty parameter $y_{\rm C}$. For the stellar mass-halo mass relation, we follow [1] and assume it to be a lognormal distribution whose median follows a power law with slope β^{M_*}, reference mass $M_0^{\rm hof}$ and a constant $\mathcal{N}$ [26],

$$M_* = M\,\mathcal{N}\left(\frac{M}{M_0^{\rm hof}}\right)^{\beta^{M_*}}, \tag{11}$$

and whose scatter can increase at low mass [23],

$$\sigma(M) = \sigma^{M_*} + \gamma^{M_*}\log_{10}\frac{M}{10^{11}M_\odot}, \tag{12}$$

$\beta^{M_*}, \sigma^{M_*} \in [0, 2]$ [7, 23] and $\gamma^{M_*} < 0$ are parameters. M is the infall mass [26].

- $\mathcal{P}(\sigma^*_{\rm los}|R_{\rm eff}, c, M_*, M) = \delta\left(\sigma - \sqrt{\frac{G}{4}\frac{M(<R_{\rm eff}/0.75)}{R_{\rm eff}}}\right)$ is given by an estimation from [18], which depends on M and c through the mass enclosed within the 3D half-light radius $M(< r_{1/2})$ ($r_{1/2} = R_{\rm eff}/0.75$ is accurate for a wide variety of stellar distributions [18]). As in [1], we ignore scatter, as other enclosed mass approximations produce nearly identical results [15]. Due to the link between $\sigma^*_{\rm los}$ and concentration, baryonic feedback can affect our results [27, 28]. To account for this we assume an NFW profile for $M < M^{\rm core}_{\rm thres}$ and a cored profile for $M > M^{\rm core}_{\rm thres}$ following [29] (where the core size depends on the time over which a galaxy has formed stars), with $M^{\rm core}_{\rm thres}$ another parameter.

As in [1], we numerically normalize μ (the differential probability) so that $\int \mu(\sigma^{*\,\rm obs}_{\rm los}, R^{\rm obs}_{\rm eff}) {\rm d}\sigma^{*\,\rm obs}_{\rm los}\, {\rm d}R^{\rm obs}_{\rm eff} = 1$. We carry out the integrals for $\mu(\sigma^{*\,\rm obs,\,i}_{\rm los}, {\rm R}^{\rm obs,\,i}_{\rm eff})$ with the vegas package [30]. Due to the possibility of integration error and human error while computing μ, we crosscheck all computations with probabilistic sampling to ensure correctness.

Method to Compute $\mathcal{P}(N_{\rm obs})$

Finally, as in [1], we take the probability to observe $N_{\rm obs}$ satellite galaxies, $\mathcal{P}(N_{\rm obs})$, to be a negative binomial distribution with intrinsic scatter $\sigma^2_{\rm I} = 0.18$ [31] and mean

$$N_{\rm expected} = \int \mathcal{P}(\sigma^*_{\rm los}, R_{\rm eff}, c, M_*, M) {\rm d}c\, {\rm d}M_*\, {\rm d}M\, {\rm d}\sigma^*_{\rm los}\, {\rm d}R_{\rm eff}, \tag{13}$$

In other words, $\mathcal{P}(\sigma^*_{\rm los}, R_{\rm eff}, c, M_*, M)$ is normalized to the expected number of observed galaxies. Low-mass halos contribute heavily to this integral, thus there is little impact from not including the Magellanic clouds in our computations. According to [1], changing the Milky Way mass within uncertainties [20] would change $N_{\rm expected}$ by about 20% [10]. This is smaller than the total scatter of $\mathcal{P}(N_{\rm obs})$.

Final Results

Overall, our likelihood $\mathcal{L}$ is dependent upon one parameter, thermal relic mass, which describes WDM physics; and eight parameters, $(M^{\rm hof}_0, \alpha^{\rm hof}, \beta^{M_*},\ \sigma^{M_*},\ \gamma^{M_*},\ M^{\rm core}_{\rm thres},\ \sigma_{{\rm C}_\Omega},\ y_{\rm C})$, which model galaxy properties and baryonic effects. To check which WDM models match the observational data of Milky Way satellite galaxies we choose a set of parameters that serve as a benchmark,

$$(M^{\rm hof}_0 = 10^{8.35}\, M_\odot,\ \alpha^{\rm hof} = 1.31,\ \beta^{M_*} = 0.96,\ \sigma^{M_*} = 0.15,\ \gamma^{M_*} = 0,\ M^{\rm core}_{\rm thres} = 10^9\ M_\odot,\ \sigma_{{\rm C}_\Omega} = 1,\ y_{\rm C} = 1).$$

The results of using these parameter values were compared to the results of varying these parameters by hand, and no significant further minimizations of the likelihood function in Eq. 1 were found. Further work would need to be done to check if there are truly no other sets of parameter values that significantly minimize the likelihood function further for certain thermal relic mass values. We compute $\Delta(-2\ln\mathcal{L})$, the difference between each likelihood value and the minimum likelihood value, for each thermal relic mass. We also compute $\Delta(-2\ln\mathcal{L})$ by only taking the $-2\ln\mathcal{P}(N_{\rm obs})$ term in Eq 1 into account (omitting velocity contributions).

We plot the total likelihood and the velocity omitted likelihood in Figure 1:

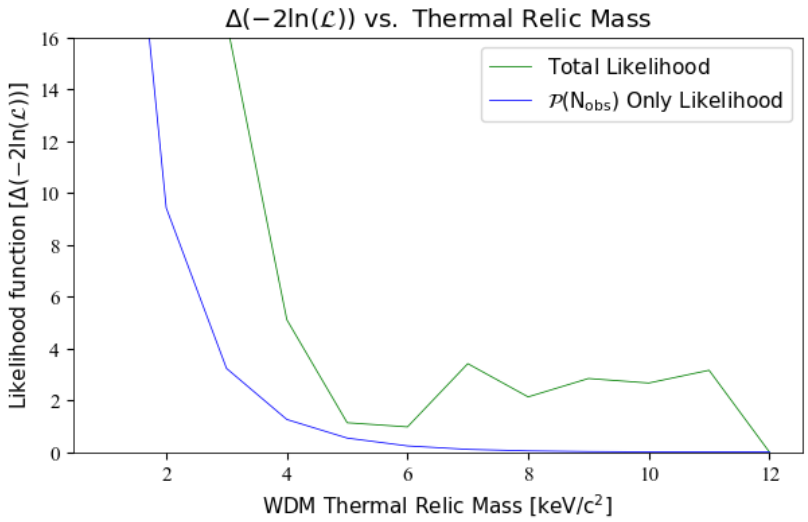

Figure 1: This figure shows the likelihood function computed using all of Eq. 1 vs. excluding velocities in Eq. 1.

We can see that the likelihood computed using only the $-2\ln\mathcal{P}(N_{\rm obs})$ term increases asymptotically at $\sim 2{\rm keV}/c^2$ where the likelihood computed including velocities increases asymptotically at $\sim 4{\rm keV}/c^2$. This means that including velocities in our calculations allowed us to improve the constraints on allowed WDM cosmologies by a factor of ~ 2.

References

[1] I. Esteban, A. H. G. Peter, and S. Y. Kim, *Milky Way satellite velocities reveal the Dark Matter power spectrum at small scales*, 2306.04674.

[2] A. W. McConnachie, *The observed properties of dwarf galaxies in and around the Local Group*, *Astron. J.* **144** (2012) 4, [1204.1562].

[3] J. F. Navarro, C. S. Frenk, and S. D. M. White, *A Universal Density Profile from Hierarchical Clustering*, **490** (Dec., 1997) 493–508, [astro-ph/9611107].

[4] G. A. Dooley, A. H. G. Peter, T. Yang, B. Willman, B. F. Griffen, and A. Frebel, *An observer's guide to the (Local Group) dwarf galaxies: predictions for their own dwarf satellite populations*, **471** (Nov., 2017) 4894–4909, [1610.00708].

[5] C. Barber, E. Starkenburg, J. Navarro, A. McConnachie, and A. Fattahi, *The Orbital Ellipticity of Satellite Galaxies and the Mass of the Milky Way*, *Mon. Not. Roy. Astron. Soc.* **437** (2014), no. 1 959–967, [1310.0466].

[6] A. S. Graus, J. S. Bullock, T. Kelley, M. Boylan-Kolchin, S. Garrison-Kimmel, and Y. Qi, *How low does it go? Too few Galactic satellites with standard reionization quenching*, **488** (Oct., 2019) 4585–4595, [1808.03654].

[7] **DES Collaboration**, E. O. Nadler *et al.*, *Milky Way Satellite Census – II. Galaxy-Halo Connection Constraints Including the Impact of the Large Magellanic Cloud*, *Astrophys. J.* **893** (2020) 48, [1912.03303].

[8] M. R. Lovell, *Towards a general parametrization of the warm dark matter halo mass function*, 2003.01125.

[9] M. R. Buckley and A. H. G. Peter, *Gravitational probes of dark matter physics*, **761** (Oct., 2018) 1–60, [1712.06615].

[10] S. Y. Kim and A. H. G. Peter, *The Milky Way satellite velocity function is a sharp probe of small-scale structure problems*, 2106.09050.

[11] A. Schneider, R. E. Smith, A. V. Macciò, and B. Moore, *Non-linear evolution of cosmological structures in warm dark matter models*, **424** (July, 2012) 684–698, [1112.0330].

[12] B. Diemer and A. V. Kravtsov, *A Universal Model for Halo Concentrations*, **799** (Jan., 2015) 108, [1407.4730].

[13] B. Diemer, *COLOSSUS: A Python Toolkit for Cosmology, Large-scale Structure, and Dark Matter Halos*, **239** (Dec., 2018) 35, [1712.04512].

[14] B. Diemer and M. Joyce, *An accurate physical model for halo concentrations*, *Astrophys. J.* **871** (2019), no. 2 168, [1809.07326].

[15] S. Y. Kim, A. H. G. Peter, and J. R. Hargis, *Missing Satellites Problem: Completeness Corrections to the Number of Satellite Galaxies in the Milky Way are Consistent with Cold Dark Matter Predictions*, **121** (Nov., 2018) 211302, [1711.06267].

[16] S. M. Walsh, B. Willman, and H. Jerjen, *The Invisibles: A Detection Algorithm to Trace the Faintest Milky Way Satellites*, **137** (Jan., 2009) 450–469, [0807.3345].

[17] S. Koposov, *et al.*, *The Luminosity Function of the Milky Way Satellites*, **686** (Oct., 2008) 279–291, [0706.2687].

[18] J. Wolf, G. D. Martinez, J. S. Bullock, M. Kaplinghat, M. Geha, R. R. Muñoz, J. D. Simon, and F. F. Avedo, *Accurate masses for dispersion-supported galaxies*, **406** (Aug., 2010) 1220–1237, [0908.2995].

[19] J. Woo, S. Courteau, and A. Dekel, *Scaling relations and the fundamental line of the local group dwarf galaxies*, **390** (Nov., 2008) 1453–1469, [0807.1331].

[20] M. Cautun, A. Benitez-Llambay, A. J. Deason, C. S. Frenk, A. Fattahi, F. A. Gómez, R. J. J. Grand, K. A. Oman, J. F. Navarro, and C. M. Simpson, *The Milky Way total mass profile as inferred from Gaia DR2*, *Mon. Not. Roy. Astron. Soc.* **494** (2020), no. 3 4291–4313, [1911.04557].

[21] V. Manwadkar and A. V. Kravtsov, *Forward-modelling the luminosity, distance, and size distributions of the Milky Way satellites*, **516** (Nov., 2022) 3944–3971, [2112.04511].

[22] E. J. Tollerud, J. S. Bullock, L. E. Strigari, and B. Willman, *Hundreds of Milky Way Satellites? Luminosity Bias in the Satellite Luminosity Function*, *Astrophys. J.* **688** (2008) 277–289, [0806.4381].

[23] S. Garrison-Kimmel *et al.*, *Not so lumpy after all: modelling the depletion of dark matter subhaloes by Milky Way-like galaxies*, *Mon. Not. Roy. Astron. Soc.* **471** (2017), no. 2 1709–1727, [1701.03792].

[24] M. Barry, A. Wetzel, S. Chapman, J. Samuel, R. Sanderson, and A. Arora, *The dark side of FIRE: predicting the population of dark matter subhaloes around Milky Way-mass galaxies*, *Mon. Not. Roy. Astron. Soc.* **523** (2023), no. 1 428–440, [2303.05527].

[25] R. D'Souza and E. F. Bell, *The infall of dwarf satellite galaxies are influenced by their host's massive accretions*, **504** (July, 2021) 5270–5286, [2104.13249].

[26] B. P. Moster, T. Naab, and S. D. M. White, *Galactic star formation and accretion histories from matching galaxies to dark matter haloes*, *Mon. Not. Roy. Astron. Soc.* **428** (2013) 3121, [1205.5807].

[27] J. I. Read and G. Gilmore, *Mass loss from dwarf spheroidal galaxies: The Origins of shallow dark matter cores and exponential surface brightness profiles*, *Mon. Not. Roy. Astron. Soc.* **356** (2005) 107–124, [astro-ph/0409565].

[28] R. Errani, J. F. Navarro, J. Peñarrubia, B. Famaey, and R. Ibata, *Dark matter halo cores and the tidal survival of Milky Way satellites*, *Mon. Not. Roy. Astron. Soc.* **519** (2022), no. 1 384–396, [2210.01131].

[29] J. I. Read, O. Agertz, and M. L. M. Collins, *Dark matter cores all the way down*, *Mon. Not. Roy. Astron. Soc.* **459** (2016), no. 3 2573–2590, [1508.04143].

[30] G. P. Lepage, *Adaptive multidimensional integration: VEGAS enhanced*, *J. Comput. Phys.* **439** (2021) 110386, [2009.05112].

[31] M. Boylan-Kolchin, V. Springel, S. D. M. White, and A. Jenkins, *There's no place like home? Statistics of Milky Way-mass dark matter haloes*, **406** (Aug., 2010) 896–912, [0911.4484].